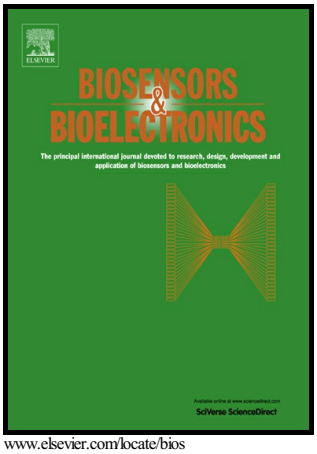

www.elsevier.com/locate/bios

An Efficient Strategy to Assemble Water Soluble Histidine-Perylene Diimide and Graphene Oxide for the Detection of PPi in Physiological Conditions and *in vitro*

B. Muthuraj, Sudip Mukherjee, Sayan Roy Chowdhury, Chittaranjan Patra, Parameswar K. Iyer

PII: S0956-5663(15)30684-9
DOI: http://dx.doi.org/10.1016/j.bios.2015.12.036
Reference: BIOS8266

To appear in: *Biosensors and Bioelectronic*

Received date: 14 August 2015
Revised date: 5 December 2015
Accepted date: 14 December 2015

Cite this article as: B. Muthuraj, Sudip Mukherjee, Sayan Roy Chowdhury Chittaranjan Patra and Parameswar K. Iyer, An Efficient Strategy to Assemble Water Soluble Histidine-Perylene Diimide and Graphene Oxide for the Detection of PPi in Physiological Conditions and *in vitro*, *Biosensors and Bioelectronic* http://dx.doi.org/10.1016/j.bios.2015.12.036

An Efficient Strategy to Assemble Water Soluble Histidine-Perylene Diimide and Graphene Oxide for the Detection of PPi in Physiological Conditions and in vitro

B. Muthuraj,[a] Sudip Mukherjee,[b,c] Sayan Roy Chowdhury,[a] Chittaranjan Patra,*[b,c] and Parameswar K. Iyer*[a,d]

[a]Department of Chemistry, Indian Institute of Technology Guwahati-781039, Assam. India. pki@iitg.ernet.in

[b]Biomaterials Group, CSIR-Indian Institute of Chemical Technology, Uppal Road, Tarnaka, Hyderabad - 500007, Telangana State, India.

[c]Academy of Scientific and Innovative Research (AcSIR), 2 Rafi Marg, New Delhi, India.

crpatra@iict.res.in; patra.chitta@gmail.com

[d]Center for Nanotechnology, Indian Institute of Technology Guwahati-781039, Assam. India.

Keywords: Inorganic phosphate; Cancer; Biosensor; Graphene oxide; perylene diimide; histidine; copper; nanocomposite

Abstract

A strategy to develop water soluble, biocompatible nanocomposite probe for the detection of pyrophosphate (PPi) in physiological conditions and in in vitro live melanoma cancer cells (B16F10) is reported. The self-assembled nanocomposite probe comprised of amino acid (histidine) functionalized perylenediimide (PDI-HIS), copper ion and graphene oxide (GO) and that could be utilized as a highly effective sensing platform in biological conditions and cellular environment via fluorescence "turn-on" for PPi detection. This controlled fabrication of metal organic self-assembled spheres along with GO proved very valuable for the detection of PPi in unprecedented sensitivity over other competing ions. The PDI-HIS-Cu-

GO (PCG) nanocomposite sensor provides a unique platform for the fluorogenic detection of PPi having a very low limit of detection (LOD) of 0.60×10^{-7} M based on the strong affinity (1.0×10^{6} M^{-1}) between the copper complex of PDI-HIS receptor and PPi. The intracellular detection of PPi using PCG also carried out in B16F10 cells where >10 times sensitively observed as compared to the PDI-HIS+Cu^{2+} complex. Thus early cancer detection via PPi recognition in physiological conditions and in live cells was possible using PCG. Furthermore, the fabrication of PDI-HIS and PCG with PVA hydrogel films and on thin layer chromatography plates demonstrated the practical utility for the detection of PPi anions by "off-on" response rapidly in a label free manner.

1. Introduction

Detection of pyrophosphate anion (PPi) has become an important area of research due to its chemical and biological significance especially in early cancer diagnosis (Hargrove et al., 2011; Rurack and Resch-Genger, 2002; Beer and Gale, 2001; Martínez-Máñez and Sancenón, 2003; Hirose et al., 1997; Ronaghi et al., 1998; Kim et al., 2010; Bhowmik et al., 2014). Among anions, pyrophosphate (PPi) is involved in numerous biological processes such as cellular metabolism (Farre et al., 2000), DNA and RNA polymerization (Steinberg et al., 2008), ATP hydrolysis (Heinonen, 2001) and enzymatic reactions (Steinberg et al., 2008). Excess PPi is responsible for rheumatologic disorders such as chondrocalcinosis or calcium pyrophosphate dihydrate (CPPD) crystal deposition disease (Wright and Doherty, 1997; Tsui, 2012). Therefore monitoring the concentrations of PPi in aqueous solutions at very low concentrations is vital for early cancer detection (Bhowmik et al., 2014; Zapata et al 2008). Till date, few sensors for PPi have been developed (Zhu et al., 2012; Liu et al., 2013; Su et al., 2013), such as turn "off-on" or "on-off" sensor in physiological conditions (Lee et al., 2015; Feng et al., 2012; Wang et al., 2014; Sokkalingam et al., 2012; Chen et al., 2011; Yu et al., 2013; Hai et al., 2015; Zhang et al., 2011; Su et al., 2009; Zhu et al., 2014; Pathak et al., 2012), indicator displacement approach (Fabbrizzi et al., 2002; McDonough et al 2006), competitive binding with metal ion (Zhao et al., 2007), metal-ligand interactions, and cancer diagnosis based on PPi detection (Bhowmik et al., 2014; Zapata et al 2008). It still remains one of the most attractive and challenging tasks to find new and smarter approaches that could improve the selectivity, sensitivity and simplicity of PPi detection in vitro and at physiological conditions.

Nanomaterials possess excellent optical, electrical, catalytic and magnetic properties compared to other bulk materials (Pankhurst et al., 2003; Alivisatos, P. 2003). To this end, the construction of nanomaterials based platforms through a self-assembly method offers not just an alternative but a powerful strategy to address and develop important nanobiosensors which avoids and overcomes complicated synthesis steps (Giljohann and Mirkin, 2009; Jin et al., 2003; Liu et al., 2002). Recently, graphene as an alternative material, has received immense attention in materials science, biotechnology and biosensors because of its unique two-dimensional nanostructure and high surface area (Novoselov et al., 2004; Allen et al., 2010). The graphene-based biosensor and biochemical analysis were performed successfully by using the chemically modified graphene oxide nanomaterials (Geim, 2009; Liu et al., 2012; Huang and Liu, 2012; Chen et al., 2012; Wang et al., 2009; Liu et al., 2008; Chang et al., 2010; Zhang et al., 2015; Gao et al., 2015; Ju et al., 2014; Ju and Chen, 2014; Zhang and Chen, 2014). Since, chemically modified graphene oxide (GO) (Novoselov et al., 2004) has promising optical and electrical properties, good water solubility and low toxicity, they are prominent materials for the development of biocompatible sensors (Georgakilas et al., 2012; Morales-Narváez and MerkoçI, 2012; Feng et al., 2013; Li et al., 2012; Xu et al., 2014; Pei et al., 2012; Liu et al., 2013). In particular, GO has been explored as a universal quencher for organic fluorescent probes (Morales-Narváez and MerkoçI, 2012; Lu et al., 2009; Balapanuru et al., 2010; Jang et al., 2010; Piao et al., 2011). Therefore, developing GO fluorescence-based optical biosensors for selective detection of target via "turn-on" analysis remains a tough task yet is of great interest. As a result, GO-based fluorescence "off-on" sensors for the detection of DNA, proteins and enzymes have been explored (Geim, 2009; Liu et al., 2012; Nel et al., 2009; Wang et al., 2010; Jung et al., 2010; Wang et al., 2011; Liu et al., 2012; Zhang et al., 2013; He et al., 2010). Recent reports demonstrate that two-dimensional GO nanomaterials are prime choice for the analysis of DNA rather than carbon nanotubes or gold nanoparticles (Li et al., 2013). Herein, we demonstrate that amino acid functionalized perylenediimide (PDI) in presence of copper and GO can be utilized for the selective detection of PPi via fluorescence "turn-on" mechanism even in the presence of other competing phosphates and anions. By using GO we overcome the disadvantages of designing and developing newer synthetic probes that usually require tedious synthesis steps and in most cases are not selective enough for a

particular analyte. We could overcome these challenges and observed that GO interacts with PDI-HIS backbone through non-covalent π-π stacking interaction which efficiently quenches the fluorescence of perylene diimide by energy transfer mechanism (Li et al., 2013; Kim et al., 2010).

2. Materials and methods

2.1. Chemicals and instruments

All the reagents and chemicals were purchased from Aldrich Chemicals, Merck or Ranbaxy (India) and were used as received. UV-vis absorption spectra were recorded on a PerkinElmer Lambda-25 spectrometer. Fluorescence spectra were recorded on a FluoroMax-4 Spectrofluorometer-Horiba Scientific. A 10 × 10 mm quartz cuvette was used for solution spectra and emission was collected at 90° relative to the excitation beam. Deionized water was obtained from Milli-Q system (Millipore). FT-IR was recorded on a Perkin Elmer spectrometer with samples prepared as KBr pellets. Atomic force microscopy images were taken by Agilent 5500-STM instrument. DLS were measured by Zetasizer Nano series Nano-ZS90 instrument.

2.2. Synthesis

2.2.1. Synthesis of PDI-HIS

PDI-HIS was synthesized by a reaction between 3,4,9,10-perylenetetracarboxylic acid bisanhydride (500 mg, 1.27 mmol), histidine (800 mg, 3.82 mmol) and 2.0 g of imidazole which were heated at 140 °C for 8h with stirring (Supporting Material, Figure S1) (Muthuraj et al., 2015; Muthuraj et al., 2015; Kalita et al., 2015). The reaction mixture was allowed to cool to 90 °C and poured into water. Then, the mixture was acidified with 2.0 M HCl, and the precipitate was washed with water and dried under vacuum at 80 °C to give the product PDI-HIS (800 mg, 94%) (Figure S1, Supporting Material).

2.3. Preparation of stock solutions

The PDI-HIS stock solution was prepared at a concentration of 1.0×10^{-3} mL^{-1} in 10 mL H_2O. This stock solution was diluted to desired concentration for each titration in 3 mL cuvette having HEPES buffer at pH 7.4.

2.4. Preparation of cation and anion stock solutions

Each salt of anions stock solutions were prepared at the concentration of 10.0×10^{-3} mL^{-1} in 5 mL Milli-Q water. The stock solutions were diluted to the desired concentrations with Milli-Q water when needed.

2.5. AFM sample preparation

In 3 mL HEPES buffer (10 mM, pH 7.4), different samples of PDI-HIS (0.33 μM) + GO (10 μg/mL), PDI-HIS (0.33 μM) + Cu^{2+} (1.33 μM) were prepared in the absence and presence of GO (10 μg/mL) and finally PDI-HIS + Cu^{2+} + GO + PPi (0.33 μM). Further, these solutions are utilized to monitor the AFM morphology images. In that case, all the solutions were separately diluted by 10 times more and then from the diluted solutions 5 μL of all the samples were mounted onto the freshly cleaned glass slide separately and dried at room temperature overnight and then recorded by atomic force microscopy (AFM) on Agilent, Model 5500 series with non-contact mode.

2.6. Dynamic light scattering study

In 3 mL HEPES buffer (10 mM, pH 7.4), different samples for DLS measurements like, PDI-HIS (0.33 μM), GO (10 μg/mL), GO (10 μg/mL) + Cu^{2+} (1.33 μM), PDI-HIS (0.33 μM) + GO (10 μg/mL), PDI-HIS (0.33 μM) + Cu^{2+} (1.33 μM) were prepared in the absence and presence of GO (10 μg/mL) and finally PDI-HIS + Cu^{2+} + GO + PPi (0.33 μM). These solutions were further utilized to monitor the hydrodynamic particle diameter by DLS. In that case, from each solution 500 μL volumes were used to record DLS by Zetasizer Nano series Nano-ZS90 instrument.

2.7. Preparation of silica TLC plates for PPi detection:

To demonstrate practical applications with the probe, we used silica TLC plates to show distinct responses of PPi anions as compared to other phosphate anions like AMP, ADP, ATP, GTP, CTP, TTP, $H_2PO_4^{2-}$, HPO_4^{2-}, PO_4^{3-} and PPi (25 eq.). The fluorescence color of PDI-HIS (10 μM) on silica gel TLC plate changed from pink to nonfluorescent in presence of GO (10 μg/mL) and with copper (2 eq.) by turn "on−off" response. Further, the nonfluorescent PCG loaded on silica gel TLC plates changed from nonfluorescent to pink in the presence of PPi by turn "off−on" response.

2.8. Preparation of hydrogel films for PPi detection:

2g PVA [poly (vinyl alcohol)] was dissolved in Milli Q water (20 mL) and stirred at 95 °C until the PVA completely dissolved. Then, the solution of PDI-HIS (10 μM) was slowly added to the PVA solution and stirred for complete mixing. After uniform

mixing the mixture of solution was loaded onto a glass sheet and dried overnight. Similarly the hydrogels of PCG+PVA were formed in absence and the presence of PPi (25 eq.) with the mixture of PDI-HIS (10 μM), GO (10μg/mL) and copper (20 μM). After uniform mixing the mixture of hydrogels were loaded onto a glass sheet and dried overnight. Then the photographs were taken at 254 nm under UV lamp illumination for all the dried hydrogel films.

2.9. Cell culture experiments:

2×10^4 numbers of melanoma cancer (B16F10) cells were seeded in each of the 24 well plates and incubated overnight at 37 °C in a CO_2 incubator before cell imaging experiments. After 24 hours B16F10 cells were treated with 300 μg/mL of PDI-HIS and incubated overnight. Cells were washed with phosphate buffer saline (PBS, 4-5 times) and fluorescence images were taken by fluorescence microscopy (Nikon Eclipse TE2000-E) (Mukherjee et al., 2014; Modak et al., 2013). The red fluorescence images were observed with a 20X microscope objective with excitation wavelength range λ_{Ex} = 510-560 nm (green) and λ_{Em} = 605 nm (red). B16F10 cells were then treated with 10^{-3} M (1 mM) of Cu^{2+} for 3 hours and GO+Cu^{2+} for 2 hours, where concentration of Cu^{2+} is 1 mM. We prepared 10 mg/mL of GO dispersion in tris-EDTA buffer (TE) and sonicated for 2 hours in a bath sonicator. Then it was centrifuged at 5000 rpm for 10 mins at 10 °C and 50 μL of GO supernatant were used with 1 mM of Cu^{2+} for further study. After extensive washing with PBS (4-5 times), the fluorescence images of cells were taken in HBSS buffer (pH = 7.4) using red filter for detection of copper ions. Furthermore, the copper treated B16F10 cells were treated with PPi (1-20 mM) and incubated for 45 mins. The re-enhancement of fluorescence signals were observed from B16F10 cells under same excitation-emission filter (red).

2.10. Cell viability using MTT assay:

Cell viability of CHO cells treated with different volumes of PDI-HIS-GO-Cu^{2+} hybrid for 4 hours and 24 hours was carried out using MTT reagents according to standard protocol. Results were expressed as percent cell viability = {[A570 (treated cells) - background]/ [A570 (untreated cells) - background]} x 100. Cell viability assay study performed for PDI-HIS-GO-Cu^{2+} (PCG) hybrid at various doses for 4 and 24 hours

exhibited negligible cytotoxicity for PCG hybrid upto 24 hours. Thus, PDI-HIS-GO-Cu^{2+} hybrid can be used for the bio-sensing of PPi without any toxic side effects. (red).

3. Results and Discussion

The GO nano sheets were prepared by a modified Hummer's method (Marcano et al., 2010). Further, the GO solution was prepared for the experiment with a final concentration of 1 mg/mL in distilled water after sonicating the aqueous GO solutions. The characterization of GO was performed by Fourier transform infrared (FT-IR), UV-vis, Raman spectroscopy, atomic force microscopy, powder XRD (Figure S2, Supporting Material) and presented in supporting material file.

In the present work a simple strategy to self-assemble materials interconnected into aggregated networks that resulted in the development of water soluble, biocompatible nanocomposite probe for the exclusive detection of pyrophosphate (PPi) in physiological conditions and in in vitro live melanoma cancer cells (B16F10) is presented. This probe while performing PPi detection using fluorescence spectroscopy shows ~100 % dequenching "turn-on" efficiency compared to ATP and other competing phosphates. The experiments confirm that the probe is selective towards PPi (~100 %) and has negligible yet a partially positive response for ATP (~18 %) but insignificant as compared to that of PPi. This difference in selectivity among PPi and ATP is also the highest for the detection difference of PPi over all other phosphates and other existing probes in literature. The limit of detection (LOD) for PPi was calculated to be 0.60×10^{-7} M using the $3\sigma/k$ equation. Hence, the proposed PCG nanomaterial displays distinguishing and incredibly selective sensing ability for PPi over ATP with superior "turn-on" and limit of detection (LOD) of 0.58×10^{-6} M (Muthuraj et al., 2015). This is achieved by preparing an appropriate combination of GO with PDI-HIS instead of developing a new synthetic probe thereby avoiding the use of difficult synthetic and purification steps, yet achieving ~100 % "turn-on" selectivity for PPi via fluorescence responses which is very unique for GO based probes that rarely show dequenching properties. The dequenching sensing ability experiments for PPi were performed using PDI-HIS+Cu^{2+} complex without and with GO. The results confirm that the PDI-HIS fluorescence reappears (~95%) at 3.3×10^{-6} M of PPi concentration which is 10 times less efficient (LOD = 10.29×10^{-6} M) as compared with the PCG. This difference of sensing for PPi using PDI-HIS+Cu^{2+} complex with GO may be due to the formation of homogeneous self-assembly process

as compared to the PDI-HIS+Cu^{2+} complex (without GO) that forms an agglomeration. Therefore, to enhance the selectivity and sensitivity for PPi among other phosphates we utilized a unique fabrication strategy comprising amino acid (histidine) functionalized fluorescent probe with graphene oxide as discussed below to achieve unprecedented selectivity for PPi since it is a vital cancer biomarker.

3.1. Quenching study of PDI-HIS with GO and Copper

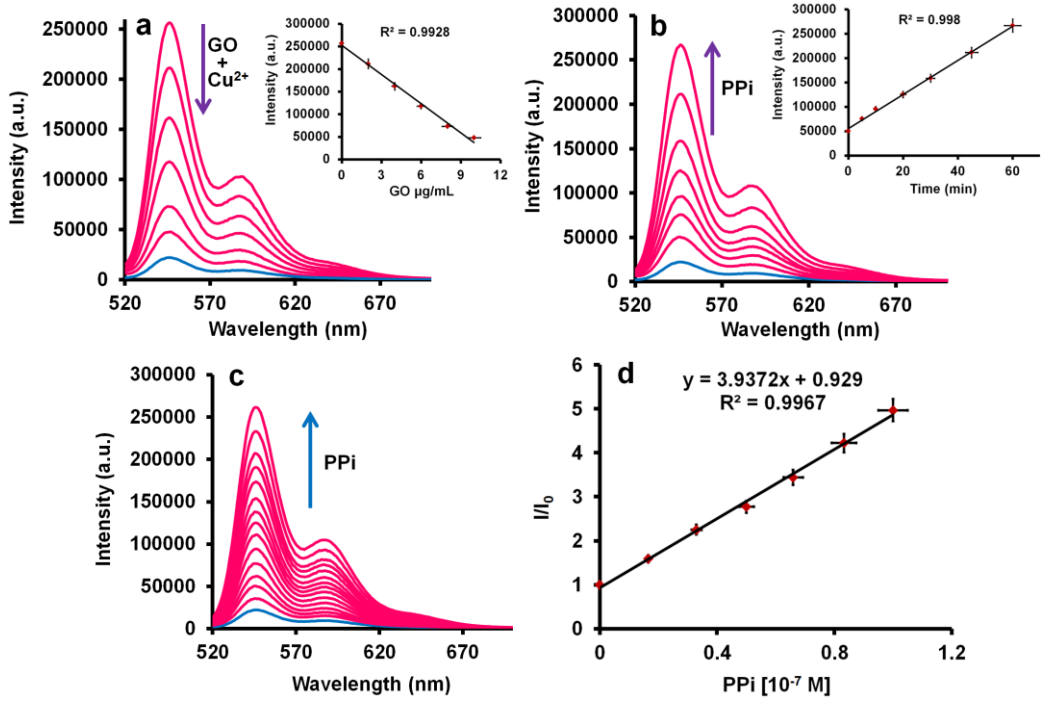

Figure 1. (a) Emission spectra of PDI-HIS (0.33 µM) upon the stepwise introduction of different amounts of GO (0-10 µg/mL) in HEPES buffer (10 mM, pH 7.4). Excitation wavelength: 508 nm. (b) Dequenching emission spectra of GO+PDI-HIS (0.33 µM) + Cu^{2+} (1.33 µM) upon the single addition of PPi (0.33 µM) at different time duration (0-60 mins). Insets in (a) Linear response in the presence of GO for the fluorescence quenching of PDI-HIS; (b) Linear response in the presence of PPi for the fluorescence dequenching of PDI-HIS. (c) Dequenching emission spectra of GO+PDI-HIS (0.33 µM) + Cu^{2+} (1.33 µM) upon the addition of PPi (0-0.33 µM) in HEPES buffer (10 mM, pH 7.4). Excitation wavelength: 508 nm. (d) Linear response observed in the presence of PPi for the fluorescence dequenching of PDI-HIS.

We evaluated the fluorescence quenching ability of GO with the histidine functionalized perylenediimide (PDI-HIS). Addition of 1-10 µg/mL GO into the highly fluorescent PDI-HIS, resulted in ~90% fluorescence quenching of PDI-HIS because of the strong π-π stacking between GO and PDI-HIS. This fluorescence

quenching is assigned to the stacking of PDI-HIS over the surface of graphene sheet, where the photo-excited energy of the electron rich PDI-HIS is transferred from the PDI fluorophore to the GO acceptor (Morales-Narváez and MerkoçI, 2012; Zhang et al., 2013; Kim et al., 2010). Further, upon addition of 1.33 μM of Cu^{2+} into the PDI-HIS+GO solution, a complete fluorescence quenching was observed in PDI-HIS due to the formation of PDI-HIS+Cu^{2+} complex on the surface of GO nano sheet. The quenching efficacy of PDI-HIS shows very good linear response in the presence of GO (1-10 μg/mL) and was observed to be R^2 = 0.9928 (Figure 1a). This optimized composition of PDI-HIS+Cu^{2+}+GO (PCG) was used as a platform for the selective detection of PPi in the present study.

3.2. Selective and sensitive detection of PPi

In the presence of 0.33 μM concentration of PPi, the maximum fluorescence of PDI-HIS at 546 nm recovered gradually with a complete recovery ratio of ~100% at time interval from 0-60 mins. (Figure 1b, the linear range of FL recovery is shown in Figure 1b, R^2 = 0.998). We ascribe the "turn-on" response of the PCG nanocomposite to the specific interactions of PPi towards Cu^{2+} ions, which causes the complex to detach from the GO surface (weak π-π stacking). The release of the complex from the GO surface leads to the fluorescence recovery of the probe, since the fluorescence quenching of PDI-HIS by GO surface was now not possible. However, the complete fluorescence recovery of PDI-HIS indicates that PPi is very selective and sensitive to break the very strong π-π stacking of PCG. Therefore, it can be concluded that this fluorescence recovery is mainly due to the PDI-HIS desorption from GO nano sheet exclusively by PPi which demonstrates a powerful affinity for Cu^{2+} ions leading to the decomplexation of PDI-HIS+Cu^{2+} complex. Similarly, on performing the titration experiment at different concentrations of PPi with PCG nanocomposite, we confirmed that the fluorescence of PDI-HIS reappeared (Figure 1c, d). The limit of detection (LOD) for PPi was calculated to be 0.60×10^{-7} M using the 3σ/k equation (Figure S3, Supporting Material) (Muthuraj et al., 2015; Muthuraj et al., 2014; Hussain et al., 2015).

To evaluate the selectivity of PCG towards PPi, we carried out the fluorescence titration with other anions including F^-, Cl^-, Br^-, I^-, $CH_3CO_2^-$, CN^-, HPO_4^{2-}, NO_3^-, NO_2^-, SO_4^{2-}, S^{2-}, HSO_4^-, Pi, AMP, ADP, ATP, GTP, CTP and TTP under identical conditions. Figure 2 confirms that the probe is most selective towards PPi (~ 100%) and has negligible yet a partially positive response for ATP (~18%) but insignificant as compared to that of PPi. This difference in selectivity for PPi over ATP is highest for any existing probe and represents the

first example of "turn-on" detection of PPi (or any anions) using GO nanocomposites. In addition to the fluorometric detection of PPi, it was also possible to visualize the color changes of PDI-HIS in presence of GO, Cu^{2+} and PPi via naked eye observation and under a hand held UV lamp illumination (at 254 nm). In presence of GO and Cu^{2+}, the pink color of PDI-HIS (yellow color under UV lamp illumination) disappeared. However, the original color of PDI-HIS is regained significantly in the presence of PPi by colorimetric method (Inset-Figure 2). Furthermore, the effect of dequenching was observed for PCG with other anions and likely competing phosphates such as Pi, ADP, AMP, GTP, CTP, TTP were insignificant and calculated to be <10%. (Figure 2; Figure S4 and S5, Supporting Material). For the control studies, we performed the dequenching sensing ability experiment by PPi without GO (only with PDI-HIS+Cu^{2+} complex). The results confirm that the PDI-HIS fluorescence reappears (~ 95%) at a PPi concentration of 3.3×10^{-6} M (10 times higher than PCG) and the LOD was found to be 10.29×10^{-6} M (Figure S3, Supporting Material) (Muthuraj et al., 2015; Muthuraj et al., 2014; Hussain et al., 2015). Similarly, upon addition of different concentrations of PPi (0-3.3 μM) into PDI-HIS+GO composite in the absence of Cu^{2+} ion, the fluorescence of PDI-HIS is not regained significantly that strongly supports that PCG is selective towards PPi anion (Figure S6, Supporting Material). Finally, the apparent binding constant was evaluated using Benesi−Hildebrand (B−H) plot by observing the fluorescence spectral changes at 546 nm for the "turn-on" detection of PPi with PDI-HIS-Cu^{2+} complex and PCG complex which are estimated to be 2.85×10^5 M^{-1} and 1.0×10^6 M^{-1} respectively (Figure S7, Supporting Material). These results confirm that PCG composite detects PPi with a very low LOD of 0.60×10^{-7} M and is more selective and efficient as compared to PDI-HIS-Cu^{2+} signifying the vital role of GO for the selectivity for PPi.

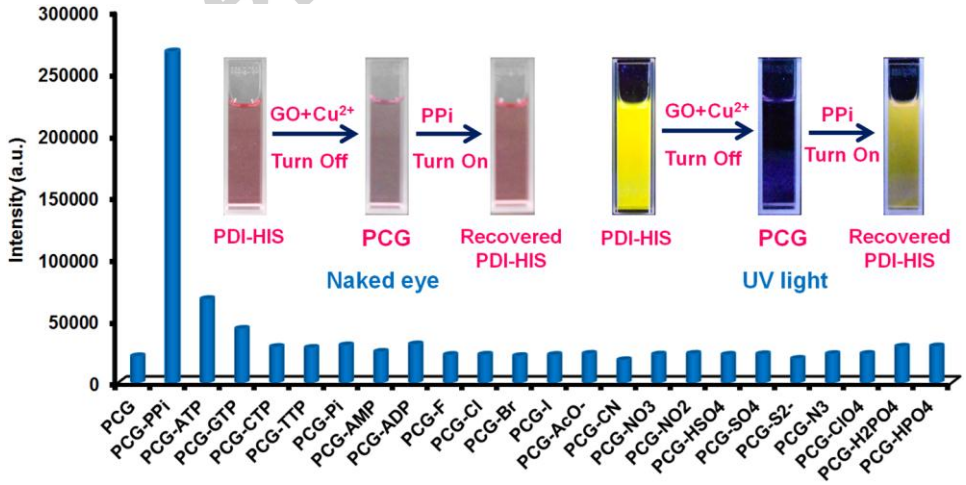

Figure 2. Bar diagram of fluorescence changes observed in the fluorescence peak of PCG in presence of various anions like PPi, ATP, Pi, AMP, GTP, CTP, TTP, ADP, F^-, Cl^-, Br^-, I^-, $CH_3CO_2^-$, CN^-, NO_3^-, NO_2^-, HSO_4^-, SO_4^{2-}, S_2^-, N_3, ClO_4^-, $H_2PO_4^{2-}$, and HPO_4^{2-} (0.33 μM). Inset: Colorimetric study of PDI-HIS (10 μM) in the absence (Pink color) and the presence (purple color) of Cu^{2+} (20 μM) with GO (10 μg/mL) and PDI-HIS+GO+Cu^{2+} with PPi (Pink color) (Under naked eye). Colorimetric study of PDI-HIS (10 μM) in the absence (yellowish orange color) and the presence (non fluorescent purple color) of Cu^{2+} (20 μM) with GO (10 μg/mL) and PCG with PPi (yellowish orange color) (UV-lamp at 254 nm).

3.3. UV-Visible studies of PDI-HIS

The self-assembly of the resultant PCG and its disassembly was examined and that was carefully studied from the absorption spectra. Figure 3A (a), illustrates that the PDI-HIS (2.5 μM) has two absorbance maximum peaks at 535 and 504 nm in HEPES buffer (10 mM, pH 7.4) solution. Further, the absorbance peaks of PDI-HIS were enhanced at 534 and 502 nm after the addition of GO (10 μg/mL) due the interactions of π electrons among them. Upon addition of Cu^{2+} solution into the PDI-HIS+GO mixtures the absorption band of PDI-HIS decreases with red shifted band at 508 nm and a new broad shoulder that appeared at ~554 nm, indicating the formation of PCG nano aggregates. Then, the PCG nano aggregates were disassembled upon addition of PPi anions as seen from the changes in the absorption spectra (Figure 3A (a)). Further, we performed the concentration dependent UV-Visible spectroscopy to understand the formation of nanoaggregates (PCG) and its disaggregation. Figure 3A (b) shows that the absorption spectra of GO (10 μg/mL) mixed PDI-HIS (1.5 μM) gives two enhanced absorbance bands at 533 and 502 nm in HEPES buffer (10 mM, pH 7.4) solution. Upon addition of Cu^{2+} solution upto 0-2 equivalents (0-3 μM), the absorption bands of PDI-HIS decreased with a red shifted band at 508 nm and a new broad shoulder appeared at ~554 nm due to the formation of π–π stacking among perylene moieties over the GO and extended to the oligomer formations into the PCG nanoaggregates (Figure 3A (b)) (Wang and Yu, 2010; Balakrishnan et al., 2005; Balakrishnan et al., 2006; Herrikhuyzen et al., 2004). Further, the PCG nanoaggregates are disassembled upon gradual addition of PPi anions which induces the reappearance of absorbance bands at 533 and 502 nm (Figure 3A. c). Finally, this result indicates the formation of PDI-HIS monomer molecules that lead to the enhancement of 533 nm absorption bands. Moreover, it is clearly evident that upon gradual addition of PPi anion (25eq.) (Figure 3A. c), a shoulder at 554 nm absorption band which is associated with the PCG nanoaggregates disappear and the ~533 and 502 nm peaks regained

gradually due to the free PDI-HIS molecules which is depicted in a proposed mechanism (Scheme 1).

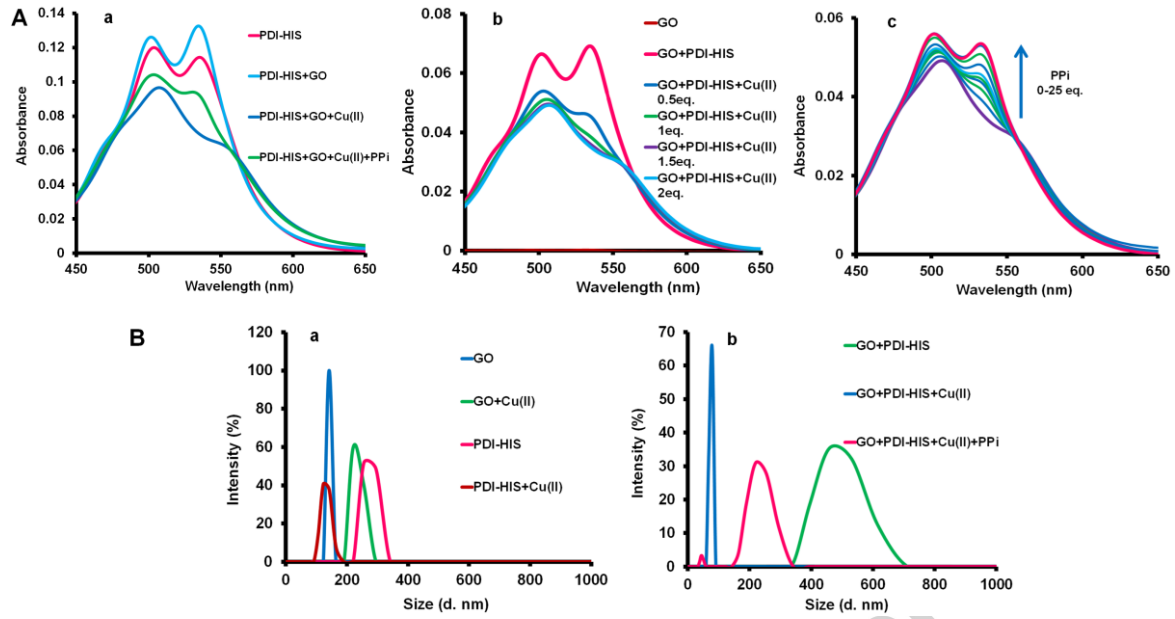

Figure 3. A (a) Absorption spectra of PDI-HIS, PCG aggregates and PCG with PPi anions in HEPES buffer solution (10 mM, pH 7.4). (b) Absorption spectra of PDI-HIS (1.5 µM) was red shifted due to the aggregation upon the addition of GO (10 µg/mL) with Cu^{2+} (3 µM) in HEPES buffer solution (10 mM, pH 7.4). (c) Absorption spectra for GO (10 µg/mL) mixed PDI-HIS (1.5 µM) with Cu^{2+} (3 µM) aggregated composites was disaggregated after the gradual addition of PPi (25 eq.) in HEPES buffer solution (10 mM, pH 7.4). B (a) DLS-based particle size analysis of GO, GO+Cu^{2+}, PDI-HIS and PDI-HIS+Cu^{2+} in HEPES buffer at pH 7.4. (b) DLS-based particle size analysis of GO+PDI-HIS, GO+PDI-HIS+Cu^{2+} and GO+PDI-HIS+Cu^{2+}+PPi in HEPES buffer at pH 7.4.

3.4. Dynamic light scattering studies of PDI-HIS

The higher order nano assembly of the resultant PCG and its disassembly was examined by dynamic light scattering (DLS) technique. Prior to metal complexation, the PDI-HIS solution (in HEPES buffer at pH 7.4) had a hydrodynamic diameter of ca. 255 ± 40 nm (indicating single molecules) at an concentration of 0.33 µM (Figure 3B). The hydrodynamic diameter of PDI-HIS with GO is observed to be in the range of 400 to 615 nm. However, upon metal complexation the hydrodynamic diameter decreases significantly to 75 ± 5 nm for GO+PDI-HIS with 1.33 µM Cu^{2+} due to the complex formation of PDI-HIS+Cu^{2+} on the surface of GO. The hydrodynamic particles diameter of the PCG nanocomposite complex were observed to be very less as compared to the formation of PDI-HIS+Cu^{2+} complex (110-160

nm) (Figure 3B). After the addition of PPi into this PCG nanocomposite, the PPi which has a strong affinity towards cupric ion induces the decomplexation. Hence, the PDI-HIS is detached from the surface of GO and the hydrodynamic particles diameter were large and in the range from 220 ± 30 nm. As a result, the analysis of the distribution of particle sizes confirms that relatively well-defined aggregates are formed during the nano self-assembly process in the presence of copper and the GO flakes with PDI-HIS.

3.5. Proposed mechanism for PCG nanoaggregates and disaggregation

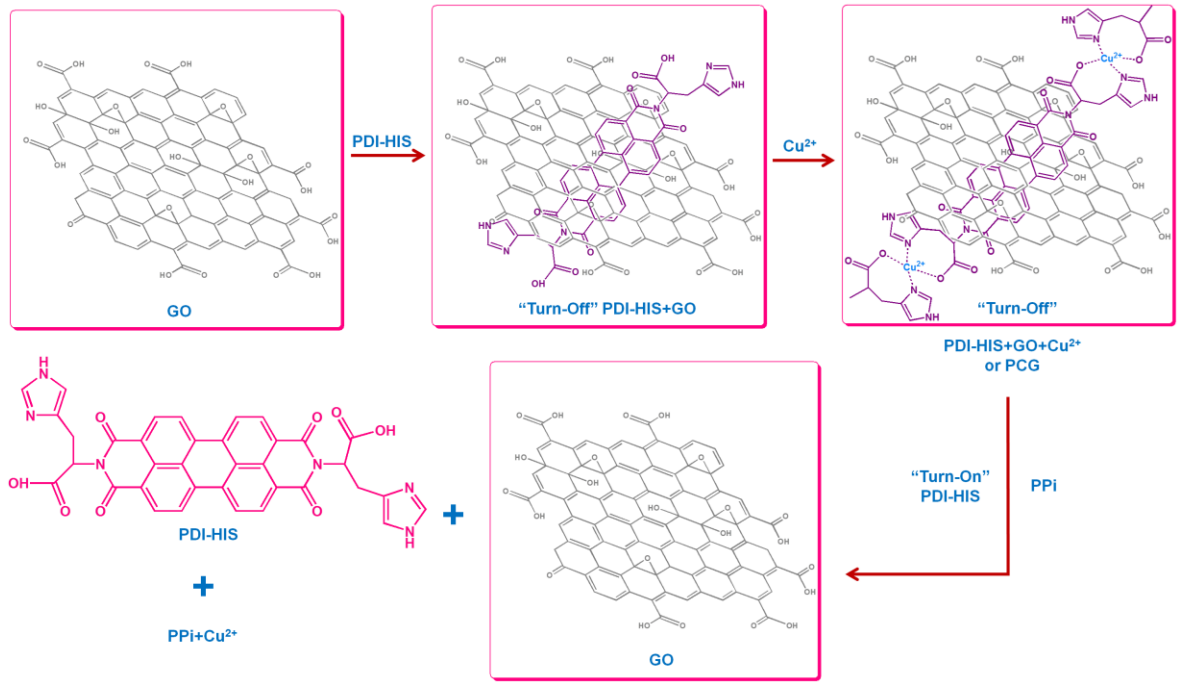

Scheme 1 Proposed mechanism for the formation of PCG nanoaggregates from the mixture of PDI-HIS, GO and Cu^{2+} and disaggregation with PPi.

3.6. AFM morphology study of PDI-HIS+Cu^{2+} with GO and PPi

As depicted in the AFM images, the morphological changes in the structural pattern of PDI-HIS differs from the in situ formed PDI-HIS+Cu^{2+} derivatives in the absence and presence of GO, which shows Cu^{2+} induced agglomeration in the absence of GO and Cu^{2+} induced homogeneous metal organic nano sphere by ordered self-assembly in presence of GO (Figure 4). In 3 mL HEPES buffer solution (10 mM, pH 7.4), different samples were prepared, namely, PDI-HIS (0.33 µM), PDI-HIS (0.33 µM) + GO (10 µg/mL), PDI-HIS (0.33 µM) + Cu^{2+} (1.33 µM), PDI-HIS + Cu^{2+} + GO and PDI-HIS + Cu^{2+} + GO + PPi (0.33 µM). Further, these diluted solutions were utilized to monitor the AFM morphology images. In that case, all the solutions were separately diluted by 10 times more and then from the diluted solutions 5 µL of all the samples were mounted onto the freshly cleaned glass

slide separately and dried at room temperature overnight and then recorded by atomic force microscopy (AFM) on Agilent, Model 5500 series with non-contact mode. In presence of Cu^{2+} ion PDI-HIS gives Cu^{2+}-induced agglomerate PDI-HIS+Cu^{2+} complex (Figure 4a-c), which indicates the formation of spherical shape PDI-HIS+Cu^{2+} complex mixed together to form agglomeration. When the same study was performed using GO, a homogeneous metal organic nano sphere copper complex is formed between PDI-HIS and Cu^{2+} ion in the surface of GO by ordered self-assembly process depending on the size dispersity and size ratios (Figure 4d-f). Moreover, in figure 4d-f, the self-assembled PCG was found to be with the size of 75 ± 5 nm diameters and 15 ± 5 nm heights. The PPi mixed PCG complex image (Figure 4g) shows that the PPi induced the decomplexation or disaggregation of PCG due to the disruption of π-π stacking as well as the likely detachment of PDI-HIS from the surface of GO with a height profile found to be 4-8 nm (Figure 4h-i). Further, we have confirmed that the morphology of GO+PDI-HIS samples showed no aggregation in the absence of Cu^{2+} ion and the average size of the particle diameter was found to be 900 ± 100 nm and 5 ± 1 nm height (Figure S8). These morphological structural differences of PDI-HIS+Cu^{2+} complex formation in the absence and presence of GO, may be the reason to selectively sense PPi ions which shows Cu^{2+} induced homogeneous metal organic nano sphere by ordered self-assembly in presence of GO (Figure 4d). Hence, AFM morphological images strongly support the fluorescence study results by the formation of self-assembled PDI-HIS+Cu^{2+} complex over the GO nanosheets which is decomplexed or disaggregated exclusively by PPi.

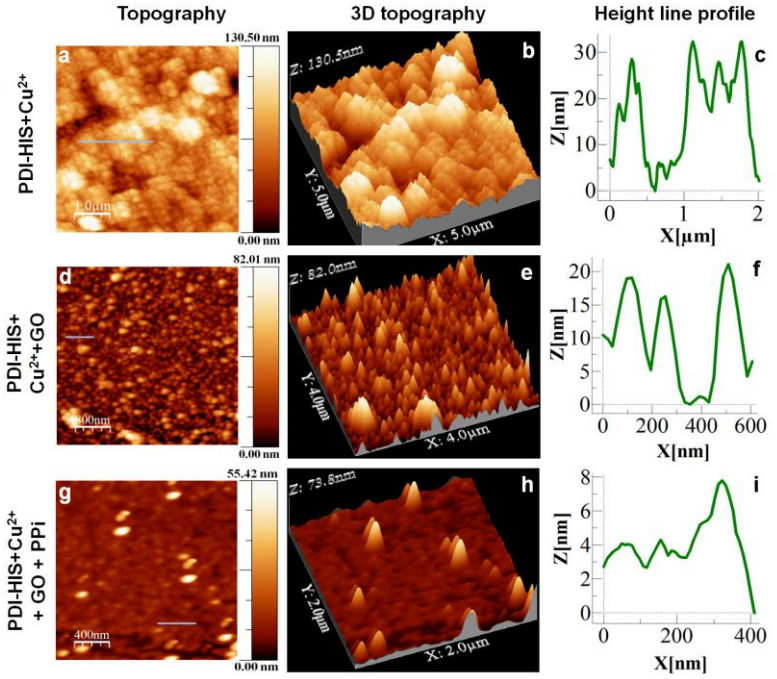

Figure 4. (a, d, g) AFM topography images of PDI-HIS+Cu^{2+} (agglomerated form), PCG (aggregated nanocomposite) and PCG+PPi (disaggregated form); (b, e, h) AFM 3D topography images of PDI-HIS+Cu^{2+} (agglomerated form), PCG (aggregated nanocomposite) and PDI-PCG+PPi (disaggregated form); (c, f, i) AFM height line profiles of PDI-HIS+Cu^{2+} (agglomerated), PCG (Nano aggregated) and PCG+PPi (disaggregated form); (X = Distance, Z = Height).

3.7. Intracellular detection of PPi in living cells by fluorescence imaging

Cell viability assay study was performed for PDI-HIS-GO-Cu^{2+} (PCG) hybrid at various doses for 4 and 24 hours that exhibited negligible cytotoxicity for PCG hybrid complex (Figure S9). Thus, PDI-HIS-GO-Cu^{2+} hybrid is biocompatible and can be used for the biosensing of PPi without any toxic side effects. We further investigated the detection of PPi in B16F10 cells using PCG composites. The B16F10 cells were seeded in each of the 24 well plates and incubated at 37 °C overnight in a CO_2 incubator prior to cell imaging studies. After 24 hours, B16F10 cells were treated with 300 µg/mL of PDI-HIS and allowed to incubate overnight to observe the images (Figure 5 and S10). Fluorescence images of B16F10 cells treated with 300 µg/mL of PDI-HIS gives bright red fluorescence which gets quenched upon incubation with Cu^{2+} (1 mM) and GO+Cu^{2+} (1 mM) (Figure 5, S10 and S11). Further, a "turn-on" red fluorescence reappeared from the B16F10 cells upon the treatment of PPi (20 mM) in case of Cu^{2+} (1 mM) treated cells but in the case of GO+Cu^{2+} (1 mM) treated cells

only 2 mM PPi (10 times less than absence of GO) was enough to generate the red fluorescence. The fluorescence reappeared in the B16F10 cells due to the disaggregation and detachment of PDI-HIS-Cu^{2+} complex from GO flakes by PPi. Finally, this result confirms that the PCG was able to detect intracellular level PPi, with much higher sensitivity than only the PDI-HIS+Cu^{2+} complex by fluorescence "turn-on" mechanism due to the disaggregation and detachment of PDI-HIS-Cu complex. This study is the first report of intracellular PPi detection using GO nanocomposites by "turn-on" fluorescence in the orange-red spectral region without the interference of other competing phosphates, especially ATP.

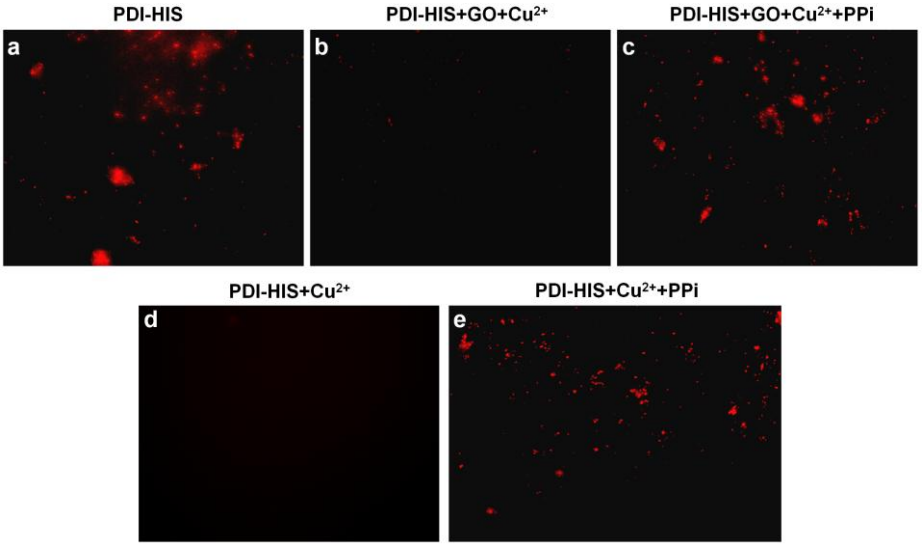

Figure 5. (a) The fluorescence image of PDI-HIS observed where PDI-HIS (300 µg/mL) incubated with B16F10 cells for 24 h (b) "Turn-off" fluorescence images observed for PCG where PDI-HIS further incubated with GO and 1 mM Cu^{2+} for 2h; (c) "Turn-on" fluorescence images observed for PDI-HIS where PCG complex further incubated with 2 mM PPi for 45 min. (d) "Turn-off" fluorescence images observed for PDI-HIS+Cu^{2+} complex where B16F10 cells incubated with PDI-HIS (300 µg/mL) and 1 mM Cu^{2+} for 2h; (e) "Turn-on" fluorescence images observed for PDI-HIS where PDI-HIS+Cu^{2+} complex further incubated with 20 mM PPi for 45 min. Excitation wavelength range λ_{ex} = 510-560 nm (green) and λ_{em} = 605 nm (red); 20X magnification.

3.8. TLC and membrane based platforms for PPi detection

To realize practical applications with this PCG nanocomposite, we performed an experiment, where the PCG was loaded onto silica TLC plates to demonstrate the sensing of PPi anions on solid platform. The silica TLC plates show a distinct response to PPi anions when compared to other phosphate anions like AMP, ADP, ATP, GTP, CTP, TTP, $H_2PO_4^{2-}$,

HPO_4^{2-}, PO_4^{3-} and PPi (25 eq.). The fluorescence color of PDI-HIS (10 μM) on silica TLC plates changed from pink to nonfluorescent (Figure 6) in presence of GO (10 μg/mL) with copper (2 eq.) by turn "on−off" response. Further, when the nonfluorescent materials of PCG were loaded on silica TLC plates it changed from nonfluorescent to pink in the presence of PPi by turn "off−on" response. Additionally, we prepared hydrogel films of desired shape and size comprising the mixtures of PVA [poly (vinyl alcohol)] and PCG to study the sensing of PPi anions. As shown in figure 6, the bright yellowish orange fluorescence color was observed for PDI-HIS+PVA hydrogels that changes from bright orange to nonfluorescent in presence of GO and Cu^{2+} ions. The nonfluorescent hydrogels of PCG+PVA showed up as bright yellowish orange fluorescent color in the presence of PPi by turn "off−on" response. These results confirmed that PCG has excellent light transmittance properties even in the form of a highly flexible hydrogel films (PDI-HIS+PVA), which has potential to be used as a portable material to sense PPi anions.

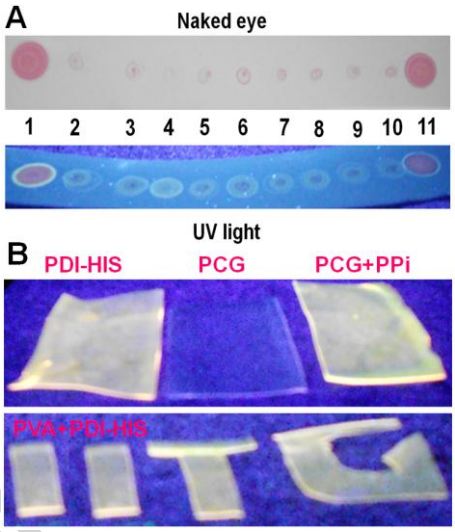

Figure 6. (A) Fluorescence color changes observed for PDI-HIS (Pink color) and PCG (purple or colorless) in the absence and presence of various phosphate anions (Pink color) on silica TLC plates observed by naked eye and UV Light at 254 nm. From left to right: 1: PDI-HIS, 2: PCG + AMP, 3: PCG + ADP, 4: PCG + ATP, 5: PCG + GTP, 6: PCG + CTP, 7: PCG + TTP, 8: PCG + H_2PO^{4-}, 9: PCG + HPO_4^{2-}, 10: PCG + PO_4^{3-}, and 11: PCG + PPi. (B) The yellowish orange fluorescence color was observed for PDI-HIS+PVA hydrogel films (UV Light at 254 nm). A nonfluoresent hydrogel film was observed for PCG+PVA and the fluorescence color reappeared for PCG+PVA hydrogel film in presence of PPi anions (UV Light at 254 nm).

4. Conclusion Sir, please reduce the conclusion

In summary, we have developed an amino acid based PDI-HIS-Cu-GO nanocomposite probe for the fluorescence "turn-on" detection of PPi in vitro and in B16F10 cells. This nanocomposite platform shows remarkable sensitivity in vitro conditions with a limit of detection of 0.60×10^{-7} M and can be used as a biomarker for early cancer diagnosis via PPi detection. The probe was found to be remarkably selective for PPi among all other biologically important phosphates including the highly interfering ATP, producing a fluorogenic "turn-on" signal response of ~100% thereby eliminating false and erroneous signals that are usually associated with assays operating on the fluorescence "turn-off" principle. This study sets the basis for the development of a new generation of probes for detection of important markers for critical diseases such as cancer by using simple and economic graphene oxide composite materials and readily available biomolecules such as amino acids appended to signal amplifying molecules thereby avoiding tedious synthetic steps for the detection of specific biological analytes that have highly competing and similar molecules in the same environment. We believe that this model PDI-HIS-Cu-GO composite sensor represents a promising sensing strategy for the detection of the biologically important phosphates and "turn-on" fluorescence response with a good linear relationship towards PPi. In a broader context, this water-soluble platform can be directly used to monitor and detect cancer and its progression via low level competitive detection of PPi. Furthermore, the fabrication of PDI-HIS and PCG with PVA hydrogel films and on TLC plates demonstrated the practical applications to detect PPi anions by "off-on" response on a solid platform.

Acknowledgements

We acknowledge the financial support from Department of Information Technology, DeitY project No. 5(9)/2012-NANO (Vol.II), Department of Science and Technology (DST), India (No. DST/TSG/PT/2009/11 & 23), (No. DST/SERB/EMR/2014/000034), DST−Max Planck Society, Germany (IGSTC/MPG/PG(PKI)/2011A/48), (SR/S2/RJN-04/2010; GAP0305) and CSIR, New Delhi (CSC0302). The CIF, IIT Guwahati is thanked for providing instrument facilities. SM thanks CSIR, N. Delhi for the Fellowship.

Appendix A. Supplementary Material

Supplementary data associated with this article can be found in the online version at doi: xxxxx.

References

Alivisatos, P., 2003, Nat. Biotechnol. 22, 47-52.

Allen, M. J., Tung, V. C., Kaner, R. B., 2010, Chem. Rev. 110, 132-145.

Balakrishnan, K., Datar, A., Naddo, T., Huang, J., Oitker, R., Yen, M., Zhao, J., Zang, L. 2006, J. Am. Chem. Soc., 128, 7390-7398.

Balakrishnan, K., Datar, A., Oitker, R., Chen, H., Zuo, J., Zang. L., 2005, J. Am. Chem. Soc., 127, 10496-10497.

Balapanuru, J., Yang, J-X., Xiao, S., Bao, Q., Jahan, M., Polavarapu, L., Wei, J., Xu, Q- H., Loh, K. P., 2010, Angew. Chem., Int. Ed. 49, 6549-6553.

Beer, P. D., Gale, P. A., 2001, Angew. Chem., Int. Ed. 40, 486-516.

Bhowmik, S., Ghosh, B. N., Marjomäki, V., Rissanen. K., 2014, J. Am. Chem. Soc. 136, 5543−5546.

Chen, D., Feng, H., Li, J. 2012, Chem. Rev. 112, 6027-6053.

Chang, H., Tang, L., Wang, Y., Jiang, J., Li, J., 2010, Anal. Chem. 82, 2341-2346.

Chen, W-H., Xing, Y., Pang, Y., 2011, Org. Lett., 13, 1362–1365.

Fabbrizzi, L., Marcotte, N., Stomeo, F., Taglietti, A., 2002, Angew. Chem., Int. Ed. 41, 3811-3814.

Farre, E. M., Geigenberger, P., Willmitzer, L., Trethewey, R. N., 2000, Plant Physiol. 123, 681-688.

Feng, L., Wu, L., Qu, X., 2013, Adv. Mater. 25, 168-186.

Feng, X., An, Y., Yao, Z., Li, C., Shi, G., 2012, ACS Appl. Mater. Interfaces 4, 614−618.

Gao, X., Lu, Y., Zhang, R., He, S., Ju, J., Liu, M., Lia, L., Chen, W., J. Mater. Chem. C, 2015, 3, 2302–2309.

Geim, A. K., 2009, Science 324, 1530-1534.

Georgakilas, V., Otyepka, M., Bourlinos, A. B., Chandra, V., Kim, N., Kemp, K. C., Hobza, P., Zboril, R., Kim, K. S., 2012, Chem. Rev. 112, 6156-6214.

Giljohann D. A., Mirkin, C. A., 2009, Nature, 462, 461-464.

Hai, Z., Bao, Y., Miao, Q., Yi, X., Liang, G., 2015, Anal. Chem. 87, 2678−2684.

Hargrove, A. E., Nieto, S., Zhang, T., Sessler, J. L., Anslyn, E. V., 2011, Chem. Rev., 111, 6603-6782.

Heinonen, J. K. Biological role of inorganic pyrophosphate, Kluwer Academic Publishers, Norwell, 2001.

Herrikhuyzen, J. V., Syamakumari, A., Schenning, A. P. H. J., Meijer, E. W., 2004, J. Am. Chem. Soc., 126, 10021-10027.

He, S., Song, B., Li, D., Zhu, C., Qi, W., Wen, Y., Wang, L., Song, S., Fang, H., Fan, C., 2010, Adv. Funct. Mater. 20, 453-459.

Hirose, M., Abe-Hashimoto, J., Ogura, K., Tahara, H., Ide, T., Yoshimura, T., 1997, J. Cancer Res. Clin. Oncol. 123, 337-344.

Huang, P-J. J., Liu, J., 2012, Anal. Chem. 84, 4192-4198.

Hussain, S., Malik, A. H., Iyer, P. K., 2015, ACS Appl. Mater. Interfaces 7, 3189-3198.

Jang, H., Kim, Y-K., Kwon, H-M., Yeo, W-S., Kim, D-E., Min, D-H., 2010, Angew. Chem., Int. Ed. 49, 5703-5707.

Jin, R., Cao, Y. C., Hao, E., Métraux, G. S., Schatz, G. C., Mirkin, C. A., 2003, Nature, 425, 487-490.

Ju, J., Chen, W., Biosens. Bioelectron., 2014, 58, 219-225.

Ju, J., Zhang, R., He, S., Chen, W., RSC Adv., 2014, 4, 52583–52589.

Jung, J. H., Cheon, D. S., Liu, F., Lee, K. B., Seo, T. S., 2010, Angew. Chem. Int. Ed. 49, 5708-5711.

Kalita, A.; Hussain, S.; Malik, A. H.; Subbarao, N. V. V.; Iyer, P. K. 2015, J. Mater. Chem. C, 3, 10767 – 10774.

Kim, J., Cote, L. J., Kim, F., Huang, J., 2010, J. Am. Chem. Soc. 132, 260-267.

Kim, J.-H., Ahn, J.-H., Barone, P. W., Jin, H., Zhang, J., Heller, D. A., Strano, M. S., 2010, Angew. Chem., Int. Ed. 49, 1456-1459.

Kim, M. J., Swamy, K. M. K., Lee, K. M., Jagdale, A. R., Kim, Y., Kim, S.-J., Yoo, K. H., Yoon, J., 2009, Chem. Commun. 7215-7217.

Lee, D. H., Kim, S. Y., Hong, J.-I., 2004, Angew. Chem., Int. Ed. 43, 4777-4780.

Lee, S., Yuen, K. K. Y., Jolliffe, K. A., Yoon, J., 2015, Chem. Soc. Rev., 44, 1749-1762.

Li, M., Yang, X., Ren, J., Qu, K., Qu, X., 2012, Adv. Mater. 24, 1722-1728.

Liu, M., Amro, N. A., Chow, C. S., Liu, G. 2002, Nano Lett. 2, 863-867.

Liu, X., Aizen, R., Freeman, R., Yehezkeli, O., Willner, I., 2012, ACS Nano 6, 3553-3563.

Liu, X., Ngo, H. T., Ge, Z., Butler S. J., Jolliffe, K. A., 2013, Chem. Sci. 4, 1680-1686.

Liu, X., Wang, F., Aizen, R., Yehezkeli, O., Willner, I., 2013, J. Am. Chem. Soc. 135, 11832-11839.

Liu, Y., Dong, X., Chen, P., 2012, Chem. Soc. Rev. 41, 2283-2307.

Liu, Z., Robinson, J. T., Sun, X., Dai, H., 2008, J. Am. Chem. Soc. 130, 10876-10877.

Li, Z., Deng, S-S., Zang, Y., Gu, Z., He, X-P., Chen, G-R., Chen, K., James, T. D., Li, J., Long, Y-T., 2013, Sci. Rep. 3, 1-7.

Lu, C-H., Yang, H-H., Zhu, C-L., Chen, X., Chen, G-N., 2009, Angew. Chem., Int. Ed. 48, 4785-4787.

Marcano, D. C., Kosynkin, D. V., Berlin, J. M., Sinitskii, A., Sun, Z., Slesarev, A., Alemany, L. B., Lu, W., Tour, J. M., 2010, ACS Nano, 4, 4806-4814.

Martínez-Máñez, R., Sancenón, F., 2003, Chem. Rev. 103, 4419-4476.

McDonough, M. J., Reynolds, A. J., Lee, W. Y. G., Jolliffe, K. A., 2006, Chem. Commun. 2971-2973.

Mizukami, S., Nagano, T., Urano, Y., Odani, A., Kikuchi, T., 2002, J. Am. Chem. Soc. 124, 3920-3925.

Modak, A., Barui, A. K., Patra, C. R., Bhaumik, A., 2013, Chem. Comm. 49, 7644-7646.

Morales-Narváez, E., Merkoçi, A., 2012, Adv. Mater. 24, 3298-3308.

Mukherjee, S., Chowdhury, D., Kotcherlakota, R., Patra, S., Vinothkumar, B., Bhadra, M. P., Sreedhar, B., Patra, C. R., 2014, Theranostics 4, 316-335.

Muthuraj, B., Chowdhury, S. R., Mukherjee, S., Patra, C. R., Iyer, P. K., 2015, RSC Adv., 5, 28211-28218.

Muthuraj, B.; Chowdhury, S. R.; Iyer, P. K., 2015, ACS Appl. Mater. Interfaces 7, 21226−21234.

Muthuraj, B., Deshmukh, R., Trivedi, V., Iyer, P. K., 2014, ACS Appl. Mater. Interfaces 6, 6562-6569.

Nel, A. E., Mädler, L., Velegol, D., Xia, T., Hoek, E. M. V., Somasundaran, P., Klaessig, F., Castranova, V., Thompson, M., 2009, Nat. Mat. 8, 543-557.

Novoselov, K. S., Geim, A. K., Morozov, S. V., Jiang, D., Zhang, Y., Dubonos, S. V., Grigorieva, I. V., Firsov, A. A., 2004, Science 306, 666-669.

Pankhurst, Q. A., Connolly, J., Jones, S., Dobson, J., 2003, J. Phys. D: Appl. Phys. 36, R167-R181.

Pathak, R. K., Tabbasum, K., Rai, A., Panda, D., Rao, C. P., 2012, Anal. Chem. 84, 5117-5123.

Pei, H., Li, J., Lv, M., Wang, J., Gao, J., Lu, J., Li, Y., Huang, Q., Hu, J., Fan, C., 2012, J. Am. Chem. Soc. 134, 13843-13849.

Piao, Y., Liu, F., Seo, T. S., 2011, Chem. Commun. 47, 12149-12151.

Ronaghi, M., Uhlén, M., Nyrén, P., 1998, Science 281, 363-365.

Rurack, K., Resch-Genger, U., 2002, Chem. Soc. Rev. 31, 116-127.

Sokkalingam, P., Kim, D. S., Hwang, H., Sessler, J. L., Lee, C.-H., 2012, Chem. Sci., 3, 1819–1824.

Steinberg, K. M., Okou, D. T., Zwick, M. E., 2008, Anal. Chem. 80, 520-528.

Su, G., Liu, Z., Xie, Z., Qian, F., He, W., Guo, Z., 2009, Dalton Trans., 7888–7890.

Su, X., Zhang, C., Xiao, X., Xu, A., Xu, Z., Zhao, M., 2013, Chem. Commun. 49, 798-800.

Tsui, F. W. L., 2012, Curr. Rheumatol. Rep. 14, 155-160.

Wang, B., Yu. C., 2010, Angew. Chem. Int. Ed., 49, 1485-1488.

Wang, J., Liu, X., Pang, Y., 2014, J. Mater. Chem. B, 2, 6634–6638.

Wang, L., Pu, K-Y., Li, J., Qi, X., Li, H., Zhang, H., Fan, C., Liu, B., 2011, Adv. Mater. 23, 4386-4391.

Wang, Y., Li, Z., Hu, D., Lin, C-T., Li, J., Lin, Y., 2010, J. Am. Chem. Soc. 132, 9274-9276.

Wang, Y., Lu, J., Tang, L., Chang, H., Li, J., 2009, Anal. Chem. 81, 9710-9715.

Wright, G. D., Doherty, M., 1997, Ann. Rheum. Dis. 56, 586-588.

Xu, J-J., Zhao, W-W., Song, S., Fan, C., Chen, H-Y., 2014, Chem. Soc. Rev. 43, 1601-1611.

Yu, C-J., Wu, S-M., Tseng, W-L., 2013, Anal. Chem. 85, 8559−8565.

Zapata, F., Caballero, A., Espinosa, A., Tárraga, A., Molina, P., 2008, J. Org. Chem. 73, 4034-4044.

Zhang, H-L., Wei, X-L., Zang, Y., Cao, J-Y., Liu, S., He, X-P., Chen, Q., Long, Y-T., Li, J., Chen, G-R., Chen, K., 2013, Adv. Mater. 25, 4097-4101.

Zhang, J. F., Park, M., Ren, W. X., Kim, Y., Kim, S. J., Jung, J. H., Kim, J. S., 2011, Chem. Commun., 47, 3568–3570.

Zhang, R., Chen, W., Biosens. Bioelectron., 2014, 55, 83-90.

Zhang, R., He, S., Zhang, C., Chen, W. J., Mater. Chem. B, 2015, 3, 4146-4154.

Zhao, X., Liu, Y., Schanze, K. S., 2007, Chem. Commun. 2914-2916.

Zhu, X., Yang, J., Schanze, K. S., 2014, Photochem. Photobiol. Sci., 13, 293-300.

Zhu, W., Huang, X., Guo, Z., Wu, X., Yu, H., Tian, H., 2012, Chem. Commun. 48, 1784-1786.

TOC

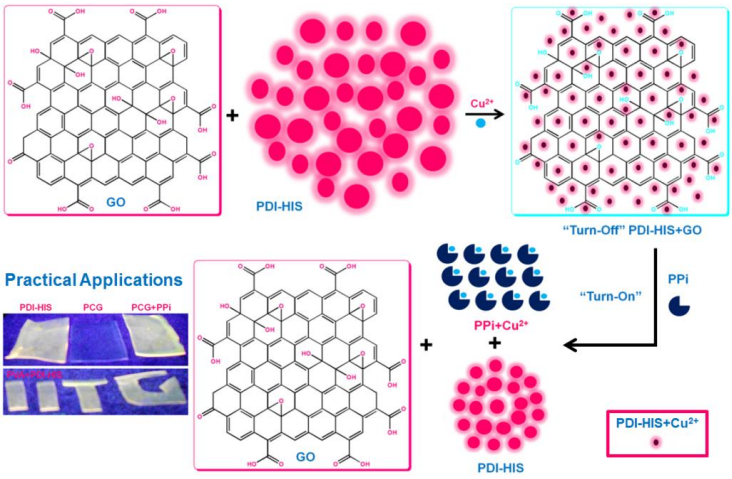

Highlights

A new biosensing platform for detection of copper(II) ion and cancer biomarker pyrophosphate (PPi) is constructed.

Histidine functionalized perylene diimide (PDI-HIS) with Cu^{2+} and graphene oxide (PCG) was used as the recognition element.

Intracellular detection of PPi using PCG was also carried out in B16F10 cells.

The fabrication of PDI-HIS and PCG with PVA hydrogel films and on thin layer chromatography plates was also demonstrated in label-free manner.